Desalination and Water Treatment
www.deswater.com

doi: 10.5004/dwt.2019.23551

144 (2019) 145–155
March

Fluoride removal from water by electrocoagulation with aluminium electrodes: effect of the water quality

Naila Ben Grich[a], Anis Attour[a,b,*], Marie Le Page Mostefa[c], Mohamed Tlili[d], François Lapicque[c]

[a]*Laboratoire de Traitement des Eaux Naturelles, Centre de Recherche et des Technologies des Eaux (CERTE), Technopole de Borj-Cedria, BP 273, 8020 Soliman, Tunisia, email: anis.attour@yahoo.fr (A. Attour)*
[b]*Institut Supérieur des Sciences et Technologies de l'Environnement, Université de Carthage, Technopole de Borj-Cedria, BP 1003, 2050 Bordj-Cedria, Tunisia*
[c]*Reactions and Chemical Engineering Laboratory, CNRS-Univ. Lorraine, BP 20451, 54000 Nancy, France*
[d]*Department of Chemistry, College of Sciences, King Khalid University, 9033 Abha, Saudi Arabia*

Received 2 July 2018; Accepted 30 November 2018

ABSTRACT

Treatment of fluoride from natural water by electrocoagulation (EC) using aluminium electrodes has been investigated in this study. The efficiency of discontinuous treatment of 10 mg F/L of two water-based fluoride solutions, after addition of sodium chloride for sufficient conductivity, has been compared. One was prepared from deionised water and the other from tap water. Although the treatment of the two solutions could be carried out with comparable electrical charge, aluminium consumption from the electrode plates depends largely on the coexisting ions. Aluminium amount dissolved on water solution depends not only on the current density but also on chloride concentration which causes electrode corrosion. Use of tap water leads to formation of inhibiting calcite film on the cathode surface due to the presence of calcium and hydrogen carbonate. At the same conductivity, treatment of tap water-based fluoride solutions required nearly two times less aluminum than that with solutions prepared with deionised water: this is to reduce the amount of aluminium sludge hydrogen carbonate-containing water, resulting in lower costs for Al plates and decreased environmental issues induced by disposal of this sludge. Experiments conducted with various current densities are discussed in terms of fluoride-over-aluminium ratio, with the support of adsorption-based EC model.

Keywords: Electrocoagulation; Aluminium; Fluoride removal; Coexisting ions; Solid characterisation; Adsorption model

1. Introduction

Fluorine is a vital element in life and human organisms. Fluoride ions can be present in drinking waters at 0.5–1 mg/L levels [1,2]: at such levels, fluoride has a positive action on skeleton and teeth reinforcement. At larger levels, these ions induce an increasing risk of dental fluorosis and progressively higher concentrations lead to severe degradation of teeth and bones (skeletal fluorosis), together with ossification of tendons and ligaments [3–6]. According to the World Health Organisation, the highest acceptable concentration in drinking waters is below 1.5 mg/L [7,8]. The US Public Service [9] has set a range of concentrations for maximum allowable fluoride in drinking water for communities based on climatic conditions. The maximum allowable fluoride concentration varied from 2.4 mg/L at 10°C to 1.4 mg/L at 32.5°C [10,11]. However, the concentration of fluoride ion can be found in groundwaters at levels higher than standards in various parts of the world, in particular in the USA, India, China, South Africa, and Northern Africa with levels from 5 to 15 mg/L

---

[*] Corresponding author.

1944-3994/1944-3986

[4,11–14]. In southern Tunisia, fluoride concentration attains 3.4 mg/L [15]. Their presence results presumably from leaching of fluorine-containing minerals by groundwaters. This species is also present in industrial wastewaters from various production sectors, e.g., semiconductors, metal processing, ceramic production, fertilisers, and glass manufacturing [4,16,17]. In particular, fluoride-containing wastewater represents 40% of hazardous wastewater produced in semiconductor industry, with fluoride concentration in the liquid waste larger than 1,500 mg/L [18].

Fluoride can be removed from (waste) waters by using various techniques, namely, (i) adsorption on solids, e.g., metal oxides, activated alumina, aluminium phosphate, calcium phosphate, or ion exchange resins [19,20], (ii) precipitation – for instance, by addition of calcium chloride or lime to produce solid calcium fluoride, in the case of heavily charged waters [21], (iii) reverse osmosis [22], and (iv) electrochemical techniques such as electrodialysis [4,22,23]. Within the last family of techniques, electrocoagulation (EC) has been often considered, in particular, because of the moderate energy demand of this technique, usually below 1 kWh/m^3 treated water.

EC is an electrochemical technique allowing the pollutant to be separated from the treated water, as adsorbed on an electrochemically generated solid. The technique has been used for decades for the treatment of various types of wastewater as for instance by Attour et al. [24,25], in the presence or abscence of a dispersed – solid or liquid – phase. The principle can be found in numerous papers: basically, metals, which can produce trivalent ions, e.g., Al and Fe, are used as electrodes in the cell [26–28]. Consider here the case of aluminium electrodes: Al^{3+} ions are generated by anode dissolution, whereas OH^- and hydrogen are formed at the cathode upon water reduction.

$$\text{Anode: } Al \rightarrow Al^{3+} + 3e^- \tag{1a}$$

$$\text{Cathode: } H_2O + 3e^- \rightarrow \frac{3}{2}H_2 + 3OH^- \tag{1b}$$

The triple-charged ions created are very efficient in changing the zeta potential of the dispersed entities (solid particles, grease droplets, micelles, liposomes) allowing their possible destabilisation, so that they can settle and/or float from the aqueous liquid. Small inorganic ions such as nitrate [29–31] and fluoride [18,32–36] can be treated by trivalent aluminium through other, more specific adsorption processes.

For pH ranging between 6 and 8, nonionic aluminium hydroxide prevails in the bulk:

$$Al^{3+} + 3OH^- \rightarrow Al(OH)_3 \tag{2}$$

Aluminium hydroxide amorphous solids occur as sweep flocs having a large surface area beneficial for a rapid adsorption and trapping of the dissolved pollutants.

Besides, the presence of chloride ions catalyses spontaneously chemical aluminium dissolution (corrosion) in water because of its negative free enthalpy difference. So, aluminium can be chemically generated from both anode and cathode, in addition to the above electrochemical reactions. Therefore, dissolution of Al usually occurs with apparent faradaic yield larger than unity.

In the present paper, focus is made on aluminium electrode dissolution. For this metal, depending on pH values, various ionic aluminium hydroxides exist: ionic species $Al(OH)^{2+}$, $Al(OH)_2^+$ – for pH in the range 3–6, and $Al(OH)_4^-$ which predominates in the liquid for alkaline pH, whereas neutral $Al(OH)_3$ prevails from pH 6 to 8. "$Al(OH)_3$", as called here, covers the various polymeric forms of neutral Al(III)-forming amorphous solids exhibiting a high affinity with water. As a matter of fact, because of the very limited solubility of $Al(OH)_3$ – $K_s = [Al^{3+}]\,[OH^-]^3 = 2.51 \times 10^{-32}$ (mol/L)^4 at 25°C [37] – trivalent aluminium is mainly in the form of a solid, as shown in Fig. 1, established from calculations reported in the Appendix. Interestingly, anionic form $Al(OH)_4^-$ represents a minor fraction of Al(III) species produced by (electro) chemical dissolution of aluminium plates, even at pH = 11 because of solubility limitation.

Literature, although abundant, is not perfectly clear on the sequence of processes allowing removal of fluoride ions from waters by EC. Electrode surface phenomena, i.e., chemical and electrochemical dissolution of aluminium, occur together with phenomena in the medium bulk involving hydroxide and fluoride ions. Hu et al. [38,39], Bennajeh et al. [40], and Essadki et al. [41], for instance, commented on aluminium hydroxides that can

- coprecipitate with fluoride to form $AlF_n(OH)_{3-n}$, where n is not necessarily an integer:

$$Al^{3+} + nF^- + (3-n)\,OH^- \rightarrow AlF_n(OH)_{3-n} \tag{3}$$

- adsorb by reacting with F^- through OH^- exchange:

$$Al(OH)_3 + nF^- \rightarrow AlF_n(OH)_{3-n} + nOH^- \tag{4}$$

Here, $AlF_n(OH)_{3-n}$ species are neutral, little soluble species, which can easily produce solids in the form of flocs or gels, that can be mechanically separated. In the above reactions, fluoride ions appear to replace hydroxide in the structure. However, because of its far weaker basicity, fluoride ions' affinity to Al(III) is lower than that of hydroxide. Hence, the fluoride ions are easily substituted by hydroxide ions [38]:

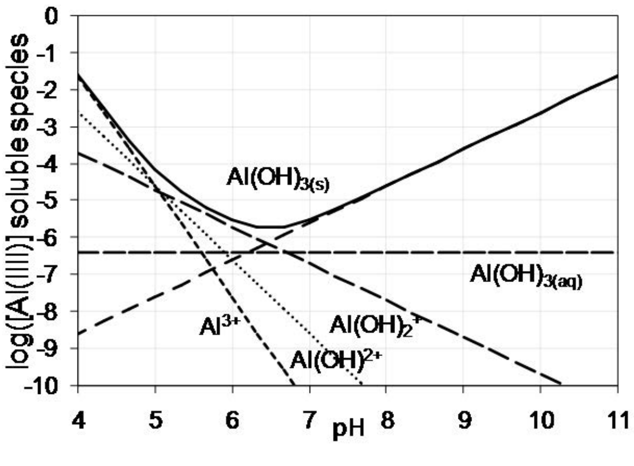

Fig. 1. Speciation of trivalent aluminium and solubility in water for [Al(III)] = 1M at 25°C.

$$AlF_n(OH)_{3-n} + nOH^- \rightarrow Al(OH)_3 + nF^- \quad (5)$$

For this reason, fluoride ions are only substituted for hydroxide ions in coordination with Al(III) if the amount of hydroxide does not suffice to neutralize the positive charge of Al(III) ions [38].

Pure and mixed neutral compounds have different solubility values: for instance, the solubility product of $AlF_2(OH)$ was determined at 3×10^{-25} $(mol/L)^4$ at 25°C [42]. Besides, all mixed fluoride-hydroxide forms of aluminium are not neutral: the existence of anionic or cationic $AlF_x(OH)_y^z$ (with the constraint $x + y + z$ below or larger than 3) has been considered in previous works, by Zhu et al. [43]. These ions can migrate to the cell electrodes and combine with electrogenerated counter-charged ions, i.e., with Al^{3+} for the anions and to OH^- for the cations. In both cases, neutral species are formed and precipitate as solids, either in neighbouring flocs or on the electrode surfaces, as evidenced by Zhu et al. [43] who found significant fluoride-containing deposits on the aluminium plates for pH larger than 7.5.

The medium pH is actually of tremendous importance in the fluoride removal yield: according to numerous studies [4,14,39,44], the optimal pH for fluoride removal is near 6 within 0.5, slightly lower than that corresponding to the lowest solubility of Al(III) in aqueous media in the range 6.5–7. Two explanations could be advanced:

- Solubility of Al mixed fluoride-hydroxide differs from that of pure Al hydroxide
- The point of zero charge (PZC) of aluminium hydroxide was measured at pH = 7.4 [14]: under this pH, aluminium hydroxide flocs with their positively charged surface adsorb fluoride ions by electrostatic forces which enhance the fluoride adsorption onto solid $Al(OH)_3$, whereas above this value, attraction of fluoride ions results only from Van der Waals forces.

In addition to pH, the presence of other species, e.g., hydrogen carbonate ions – often present in groundwaters – has been considered in combined chemical coagulation with EC by Zhao et al. [45]: the presence of this species was shown to contribute to alkalinisation of the water, in addition to reaction (1b). Best performances can then be obtained by a slight acidification of the water to compensate the presence of the weak alkaline hydrogen carbonate ions. However, the effect of HCO_3^- on fluoride removal by EC does not seem to have been investigated up to now.

The present investigation was aimed to understand the role of hydrogen carbonate ions, often present in natural water, on fluoride removal by EC, not only in terms of cell treatment performance after a given periodic time or energy but also in terms of adsorption equilibrium between Al(III) flocs and fluoride ions.

2. Materials and methods

2.1. Experimental setup

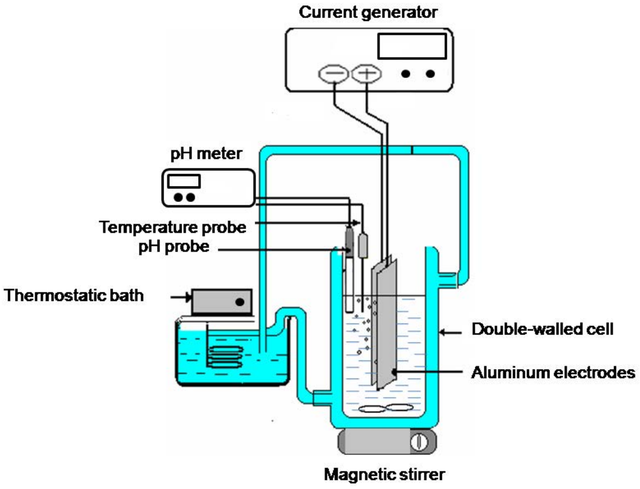

Fig. 2. Experimental setup.

Fig. 2 shows the experimental setup. Tests had been made in a stirred EC jacketed cell with a volume of 1.2 L. Two monopolar facing Al electrodes (2017A (AU4G)) were immersed in the solution with an electrochemical active area of 10 cm² × 5 cm² with a 5-mm electrode gap. The area of one side (50 cm²) has been arbitrarily considered in calculation of the current density from the current applied. The initial thickness of the aluminium plates (3 mm) allowed sufficient stability in the cell. To avoid any effect caused to the "history" of the electrodes, electrodes were polished with 400 grit superfine sandpaper, degreased, and then rinsed with distilled water after each treatment.

To avoid shearing of flocs, the stirring was kept low enough. Therefore, homogenisation of the solution was achieved with an magnetic stirrer (SBS, Paris, France) at 150 rpm. The temperature of the batch reactor was measured during the experiment and kept at 25°C by water circulation with a thermostatic bath.

The electrodes were connected to a direct current power supply (ALR 3002M) delivering a current up to 2.5 A and a voltage below 30 V. Both current and cell voltages were displayed by the generator. EC experiments were carried out under galvanostatic conditions. The current was fixed at 0.1, 0.15, and 0.25 A corresponding to current density equal to 2, 3, and 5 mA/cm², respectively. Time $t = 0$ in runs corresponds to switching on the power supply. The cell voltage and the solution pH were continuously monitored. Tests were carried out with treatment of 1 L solution along 90 min runs.

2.2. Solutions and experimental analyses

Fluoride solutions of 10 mg F^-/L were prepared by dissolving 22.1 mg of sodium fluoride (Qualikems Laboratory reagent, Gujarat, India) per litre of water. Two waters have been used:

- Local tap water:

The initial pH of the tap water was 7.8, and its conductivity at ambient temperature was 0.85 mS/cm. The pH of tap water was set to 6 upon addition of 0.1M dilute hydrochloric acid solution (Scharlau, Barcelona, Spain) to correspond to the optimal pH recommended by Shen et al. [4], Hamamoto and Kishimoto [14], and Zhu et al. [43]. To limit the ohmic drop in the cell, the conductivity of tap water was set to 2.0 mS/cm upon addition of 600 mg/L sodium chloride (Chemi-Pharma, Ariana, Tunisia). Its composition is given in Table 1.

- Deionised water:

The pH of deionised water with initial pH around 6.7 was adjusted to 6 to have similar initial pH than tap water. Sodium chloride was then added at 1,250 mg/L, so that the conductivity could attain 2.0 mS/cm and the ohmic drop in the cell would be comparable to that of tap water.

The conductivity was measured using a Mettler Toledo conductimeter (Greifensee, Suisse Switzerland). Temperature and pH were measured continuously using a pH meter (Hanna Instruments, Michigan, USA).

Samples, with a volume of 5 mL, were regularly drawn from the solution and then filtered to separate aluminium hydroxide flocs. Fluoride ions were analysed using a 781 pH/Ion Meter (Metrohm, Kolkata, India) with a selective electrode (Metrohm 6.0502.750 F) and an Ag/AgCl reference electrode according to the standard method recommended by American Public Health Association [46]: 5 mL of total ionic strength adjustment buffer solution containing CDTA (1,2-diaminocyclohexanetera-acetic acid monohydrate) (Alfa Aesar, Lancashire, United Kingdom). The CDTA can complex interfering cations and release free fluoride ions, mainly Al(III) and Ca^{2+} in the present case.

The fluoride removal efficiency (RE%) was calculated at time *t* from the fluoride concentration at initial time and time *t*, $[F^-]_0$ and $[F^-]_t$, respectively:

$$\mathrm{RE}(\%) = \frac{[\mathrm{F}^-]_0 - [\mathrm{F}^-]_t}{[\mathrm{F}^-]_i} \times 100 \tag{6}$$

The amounts of dissolved Al electrodes versus time have been determined by the following weighing method. The current generator was switched off at regular intervals; then, the two electrodes were removed from the cell, rinsed with distilled water, wiped, cleaned with paper cloth, and then weighed, before being reinstalled in the cell and further switching on the generator: the amount of Al dissolved from both electrodes was deduced from the weight difference from the initial mass of the Al plates measured by a precision balance. The uncertainty in aluminium weight was 0.1 mg.

Table 1
Composition of the tap water-based fluoride solution before and after 30 min EC at 5 mA/cm²

Ions	Before treatment (mg/L)	After treatment (mg/L)
F^-	10.6	1.02
Cl^-	550	497
HCO_3^-	61	24.4
SO_4^{2-}	56	55.2
Ca^{2+}	60.2	45.7
Mg^{2+}	48.6	39.4
Na^+	298	298
K^+	5.3	5.3

The analytical procedures used in this study were those recommended by Afnor [47]. Calcium and magnesium concentrations were obtained by ethylene diamine tetraacetic acid (EDTA) complexometry titration. HCO_3^- concentration of the sample was carried out by volumetric method by titration with 10^{-2}M hydrochloric acid in the presence of bromocresol green (as indicator) [48]. Chloride concentration was determined by titration using Mohr method [48]. Sulphates were analysed by gravimetry. Measurements of potassium and sodium concentrations were carried out by Elico CL 378 flame photometer (Telangana, India).

The mineralogical structure of solid compounds was determined by X-ray diffraction (XRD) using a Philips Panalytical X'Pert Pro in step scanning mode with CuKα source. The recorded spectra were fitted by PANalytical's High Score plus software.

3. Results and discussions

3.1. Dissolution of aluminium

The amount of aluminium dissolved from the electrodes for different current densities *i* = 2, 3, and 5 mA/cm² vs. the specific charge is plotted in Figs. 3(a) and (b) for the anode and the cathode, respectively. The anodes dissolved regularly over the runs as shown by the nearly linear variations. For each electrode, all data are gathered by the same profile. Moreover, the rate of dissolution is somewhat larger than that predicted by Faraday's law appearing in dotted line on Fig. 3(a), expressing the contribution of corrosion induced by the presence of chloride ions in the solutions. Corrosion is slightly more significant with deionised water, with an average current yield with Al at the anode approx. 18% larger than that with the tap water. As a matter of fact, the concentration of chloride in deionised water at approx. 760 mg/L is higher than that in tap water, being near 550 mg/L, which explained the different corrosion rates.

Corrosion of the cathode is often reported in EC works [12,25,26]. This phenomenon has also been observed in the present work (Fig. 3(b)). According to Picard et al. [26] and Landolt [49], aluminium cathodes are attacked by the hydroxyl ions produced locally upon water reduction during the EC process to form Al hydroxides and hydrogen. For runs conducted with tap water, all data follow the same, slowly increasing variation of Al(III) concentration from the cathode with the charge corresponding to an equivalent Al current yield at the cathode near 18%. By contrast, cathode dissolution is much more important with "deionised" water, with an equivalent current yield at the cathode ranging from 0.7 to 1.3 depending on the charge and the current density (Fig. 3(b)): the highest values of the yield have been observed with the lowest current density, presumably because of the lowest significance of faradaic phenomena. Moreover, the side corrosion was found to be more important in the first half of the runs. Replicated tests with the three current densities confirmed the various observations. The spectacular Al electroless dissolution is related to the appreciable chloride content in the solutions prepared with deionised water. Then, the cathode corrosion induced by the presence of chloride ions seems to be more important than corrosion induced by hydroxyl ions produced at the cathode.

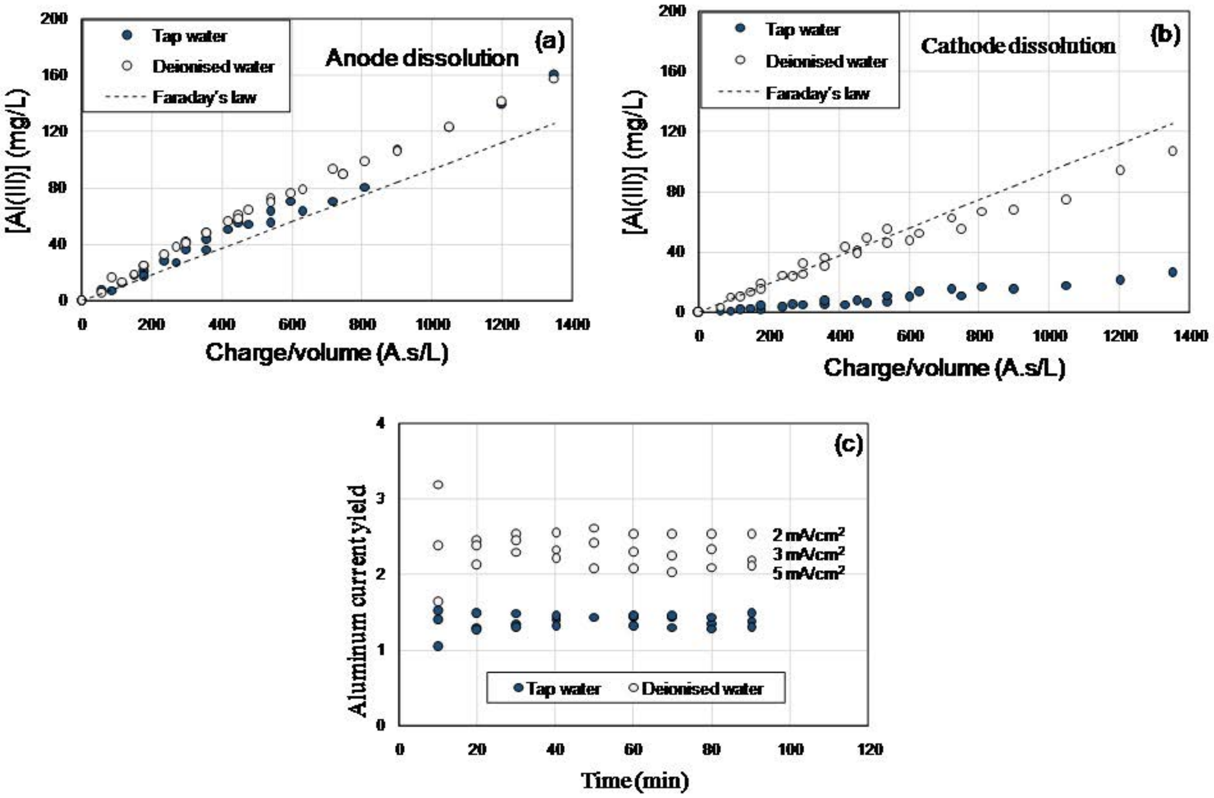

Fig. 3. Dissolution of aluminium in the electrocoagulation cells ($[F]_0$ = 10 mg/L, T = 25°C) depending on the water used and with current density i = 2, 3, and 5 mA/cm^2 (no specific symbols for the various current density levels); dotted lines are for theoretical electrochemical dissolved aluminium: (a) anode aluminium dissolution, (b) cathode aluminium dissolution versus charge over liquid volume, and (c) current efficiency of aluminium dissolution (current yield) versus time.

The overall current yield of aluminium dissolution is shown in Fig. 3(c) for the two water solutions tested. For tap water, the yield is nearly constant over the time, ranging from 1.25 to 1.5, with little effect of the current density. With deionised water, the dissolution aluminium yield follows nearly parallel trends, nevertheless lying in the range 2–2.7 (Fig. 3(c)). The very different behaviour of the aluminium plates depending on the nature of the water employed can be related to the cell voltages measured. As a matter of fact, the cell voltage was somewhat larger with tap water than with deionised water, with differences ranging from 0.1 to 0.2 V depending on the current density (data not shown). The presence of hydrogen carbonate and other ions contained in tap water may limit the strong corrosive effect of chloride on the cathode, which clearly appears with deionised water.

3.2. Efficiency of the treatment

With deionised water, pH increased rapidly along the run to values in the order of 9 (Fig. 4(a)) and then remained nearly constant because of the buffering effect of the system $Al(OH)_3$/$Al(OH)_4$. At this pH, almost 90% of fluoride was removed: as shown in Fig. 4(b), data related to the three current density levels could be well correlated to the amount of Al dissolved.

In the case of tap water, pH changes quite less in the course of the run from its initial level to 6.7, 7.5, and 8.3 for i = 2, 3, and 5 mA/cm^2, respectively (Fig. 5(a)): higher current density resulted in more important increase in pH, although to a moderate extent. The little significant change in pH can be attributed by the presence of ions contained in tap water, in particular hydrogen carbonate ions, which allow appreciable buffering of the water by reacting with hydroxide ions produced at the cathode. Moreover, removal of fluoride ions could be achieved with comparable aluminium dosage for the three current density levels investigated (Fig. 5(b)).

In addition to different pH profiles with time, the effect of water quality appears clear through the amount of aluminium required for efficient treatment near 45 mg/L with tap water but which attains nearly 140 mg/L with deionised water for 90% fluoride abatement.

This striking difference is strongly related to the different dissolution aluminium yields commented above. As a matter of fact, the data obtained are compared in terms of treatment efficiency versus the electrical charge on Fig. 6(a), combining the three current density levels for the sake of clarity. The figure clearly shows that the fluoride removal yield can be obtained with a lower charge with tap water (approx. 400 As/L) than with deionised water for which 600–700 As/L are required for comparable abatement. This can be linked to the pH variation with the charge passed versus time (Fig. 6(b)): as a matter of fact, as reported formerly, fluoride complexation by Al hydroxides is more efficient at neutral pH than in (slightly) alkaline solution [14,38].

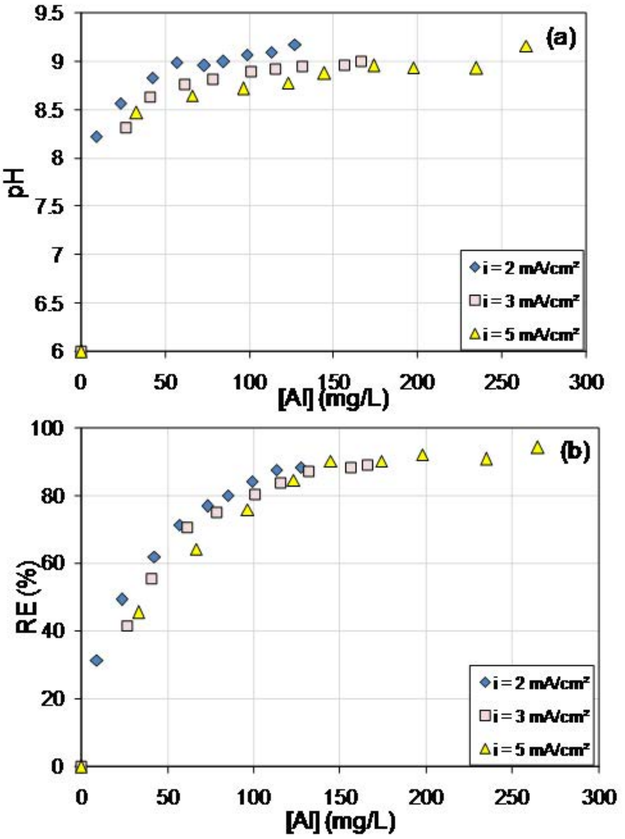

Fig. 4. Electrocoagulation treatment of deionised water-based fluoride solutions with various current densities (i = 2, 3, and 5 mA/cm^2) versus the concentration of dissolved aluminium generated in the EC cell ($[F]_0$ = 10 mg/L, T = 25°C): (a) solution pH and (b) fluoride removal yield.

Therefore, final comparison of the two treatments can be expressed as follows:

- In terms of energy consumption, fluoride removal requires from 0.1 to 0.35 kWh/m^3 – depending on the current density levels – with deionised water and approx.. 13% more with tap water, owing to the larger cell voltages reported in section 3.1 which are attributed to likely passivation of the cathode surface.
- In terms of aluminium dosage, use of deionised water induces aluminium dosage of nearly 3 times larger than that with tap water: in addition to the additional cost of the sacrificial metal plates, much more Al-based sludge is produced in the treatment of deionised water-based solutions, which is to be accounted when considering its storage issue.

3.3. Analysis of the solids and sludge formed

No deposits were observed on the anode surface as well as on the surface of the cathode used in the treatment of deionised water-based fluoride solutions. In contrast, after treatment with tap water-based fluoride solutions, optically visible deposits were formed on the cathode surface: more important solid deposits were observed with the highest current density.

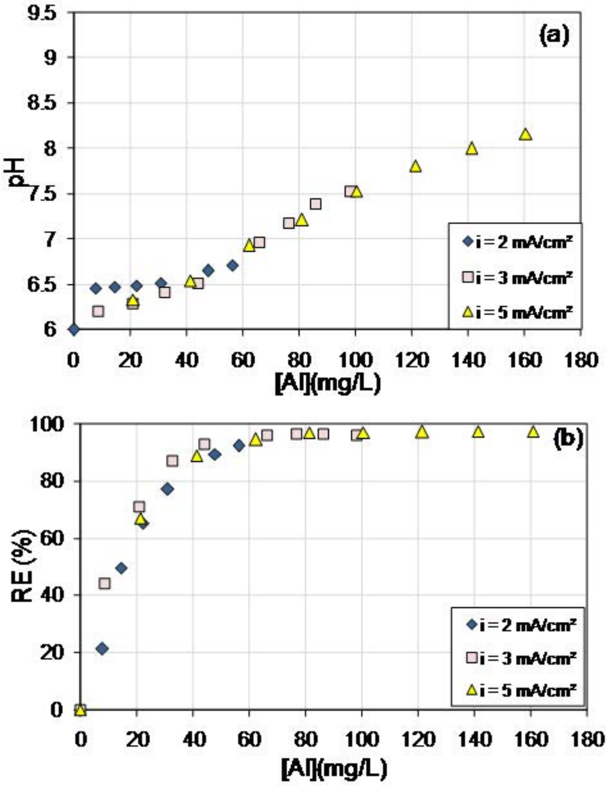

Fig. 5. Electrocoagulation treatment of tap water-based fluoride solutions with various current densities (i = 2, 3, and 5 mA/cm^2) versus the concentration of dissolved aluminium ($[F]_0$ = 10 mg/L, T = 25°C): (a) solution pH and (b) fluoride removal yield.

After recovery from the surface by scrapping, the solid deposit was submitted to XRD spectroscopy and then identified by the dedicated software. As seen in Fig. 7, XRD patterns revealed the presence of the calcite form of calcium carbonate in addition to metal aluminium coming from Al cathode.

For confirmation, formation of solids that can be generated from tap water solutions was simulated by using the PHREEQC software [50], considering the composition of the solution (Table 1) and depending on pH. Although the pH of tap water solutions changed little in the treatment, pH exhibits a significant gradient in the vicinity of the cathode surface because of OH^- production on the cathode surface together with hydrogen: upon high pH level, carbonate anions – formed from hydrocarbonate in alkaline medium – combine to calcium and magnesium cations to form little soluble solids. Simulation conducted for pH ranging from 7 to 12 shows the possible formation of Ca- and Mg-containing minerals, e.g., dolomite $CaMg(CO_3)_2$, calcite $CaCO_3$, huntite $CaMg_3(CO_3)_4$, magnesite $MgCO_3$, and brucite $Mg(OH)_2$: this last solid might be formed by magnesium hydroxide precipitation near the cathode surface. Formation of calcium and magnesium fluoride, although reported by Govindan et al. [50], was not predicted by the simulation.

XRD patterns of all possible minerals were checked and compared with the experimental spectra, but only calcite could be doubtlessly identified. Therefore, the increased

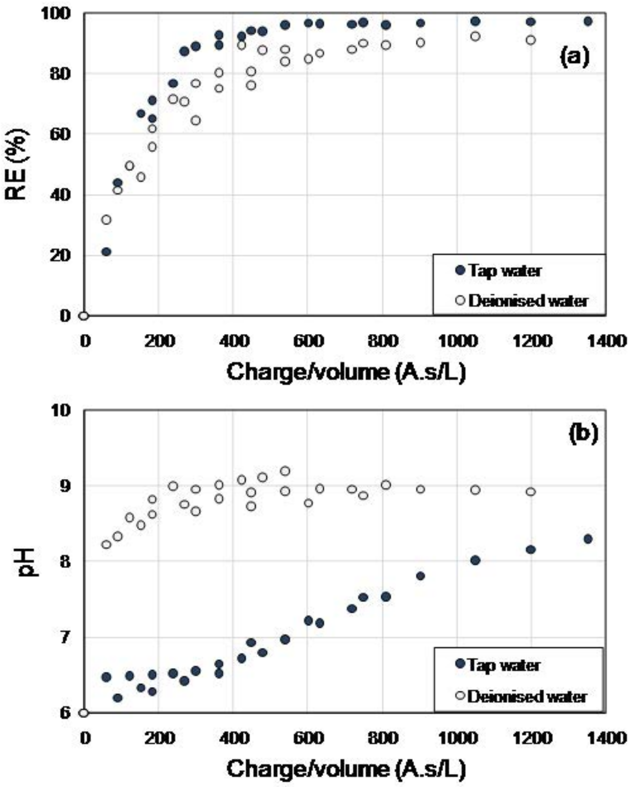

Fig. 6. Electrocoagulation treatment of deionised and tap water-based fluoride solutions with various current densities (i = 2, 3, and 5 mA/cm^2) versus charge over liquid volume ($[F]_0$ = 10 mg/L, T = 25°C): (a) fluoride removal yield and (b) solution pH.

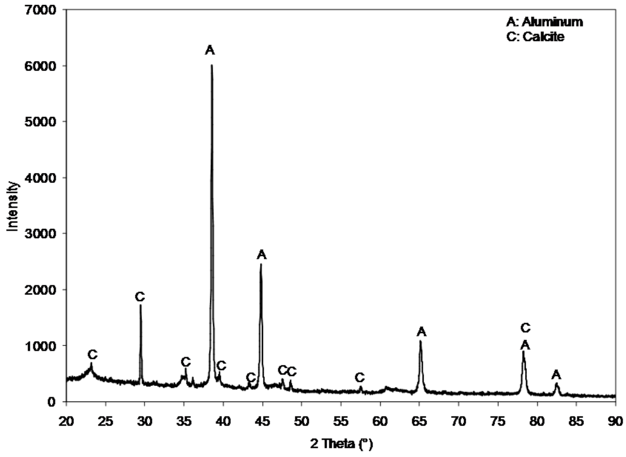

Fig. 7. XRD pattern of dried deposit formed at the cathode after treatment of tap water-based fluoride solutions ($[F]_0$ = 10 mg/L, i = 2 mA/cm^2, T = 25°C, time = 90 min).

cell voltages observed in the treatment of tap water solution were attributed to the formation of inhibiting calcite film. Analysis of calcium and magnesium after 30 min EC at 5 mA/cm^2 shows the decrease in their concentrations in solution (Table 1). This would indicate the formation of calcium/magnesium carbonates on the cathode, in agreement with the significant reduction of hydrogen carbonate ions in the EC test (Table 1). Although only calcite was clearly identified, formation of other calcium and magnesium carbonate could not be definitely excluded.

As a matter of fact, by increasing the local pH at the vicinity of cathode-electrolyte surface, the release of hydroxide ions promotes calcium carbonate precipitation by the following reactions:

$$\text{Near the cathode: } OH^- + HCO_3^- \rightarrow CO_3^{2-} + H_2O \tag{7}$$

$$\text{At the interface: } Ca^{2+} + CO_3^{2-} \rightarrow CaCO_3 \tag{8}$$

Magnesium ions can react with carbonate produced in the vicinity of the cathode-electrolyte interface to form magnesium carbonate $Mg(CO)_3$ (magnesite) or with hydroxide leading to $Mg(OH)_2$ (brucite). Huntite $Mg_3Ca(CO_3)_4$ and dolomite $CaMg(CO_3)_2$ may also be formed. Govindan et al. [51] mentioned the possible formation of nanocrystalline CaF_2 and MgF_2. The slight reduction in SO_4^{2-} concentration can be attributed to its weak adsorption on aluminium flocs. Zuo et al. [52] suggested that SO_4^{2-} has a negative effect on fluoride removal due to the ion exchange competition between SO_4^{2-} and F^-.

The composition of the sludge in the bottom of the cell, after EC experiments, was studied by XRD. XRD spectra of Al sludge produced with tap water-based solution exhibit shallow diffraction peaks revealing amorphous $Al(OH)_3$ (data not shown). In contrast, the XRD pattern of the sludge produced with deionised water shows the presence of crystalline solids. As seen in Fig. 8, the peaks at 2θ = 18.86°, 20.36°, 27.88°, 33.1°, 38.19°, 40.68°, 45.66°, 53.23°, 47.6°, 59.4°, and 63.82° were identified as being for the bayerite form of solid aluminium hydroxide $Al(OH)_3$ and not for the gibbsite form as reported by Emamjomeh and Sivakumar [53]. Moreover, the other peaks indicate the presence of aluminium fluoride-hydroxide complexes $[Al(OH,F)_3]$ formed, as explained above. Then, fluoride ions may react to form $AlF_n(OH)_{3-n}$, which should be the coprecipitate solid form.

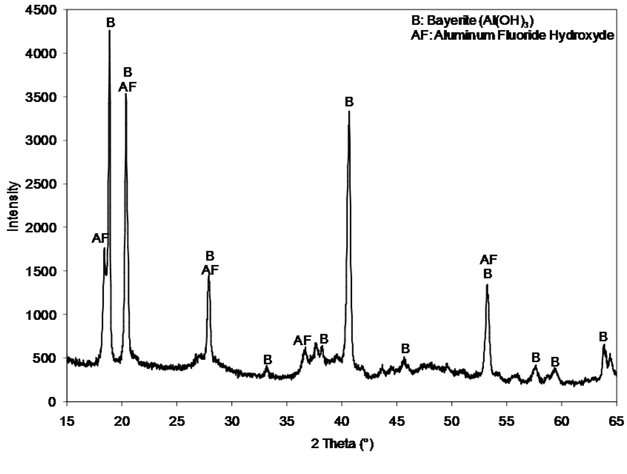

Fig.8. XDR pattern of dried settled sludge after treatment of deionised water-based fluoride solutions by electrocoagulation process ($[F]_0$ = 10 mg/L, i = 5 mA/cm^2, T = 25°C, time = 90 min).

3.4. Modelling EC runs by fluoride adsorption

The progress of fluoride ion removal by EC is due to (electro)chemical generation of aluminium species from the sacrificial electrodes, by formation of amorphous solid flocs of aluminium hydroxide $Al(OH)_3$, then by adsorption of the polluting anions on the floc surface, or by their reaction with aluminium and hydroxide species. Even though dynamic models combining Al (III) electrochemical generation and fluoride adsorption have been formerly developed [39,54], it has been preferred to use a previously published model [55] considering adsorption equilibrium between a given amount of Al(III) flocs and the polluting species: this implicitly means that the physicochemical steps in liquid phase mentioned above are fast processes.

Therefore, the solid sorbent, with an equivalent total aluminium concentration $[\text{Al}]_t$, can be free Al_f or combined to fluoride ions, written here "Al-F", regardless of the molar or weight ratio between F and Al elements in the complex form. Mass balance in trivalent (solid) Al is then written as

$$\left[\text{Al}\right]_t = \left[\text{Al}\right]_f + \left[\text{Al}-\text{F}\right] \tag{9}$$

Adsorption equilibrium is represented by constant K defined as

$$K = \frac{\left[\text{Al}-\text{F}\right]}{\left[\text{Al}\right]_f \left[\text{F}\right]} \tag{10}$$

where [F] is the concentration of non-bound fluoride, i.e., the concentration value obtained by potentiometric analysis with the specific electrode. Moreover, mass balance on fluoride species is written as

$$\left[\text{F}\right]_0 = \left[\text{F}\right] + n\left[\text{Al}-\text{F}\right] \tag{11}$$

where subscript 0 corresponds to initial time. Coefficient n is expressed in mg F/L per mg solid Al/L or in mg F per mg solid Al. Combination of Eqs. (9)–(11) leads to

$$K\left[\text{F}\right]^2 + \left[\text{F}\right]\left[1 + \text{K}\left(n\left[\text{Al}\right]_t - \left[\text{F}\right]_0\right)\right] - \left[\text{F}\right]_0 = 0 \tag{12}$$

from which the concentration of remaining fluoride ions can be calculated from the amount of Al(III) generated. Besides, upon rearrangement of Eqs. (9) and (10), the following relationship can be obtained:

$$\left[\text{Al}-\text{F}\right] = \frac{K\left[\text{Al}\right]_t\left[\text{F}\right]}{1 + K\left[\text{F}\right]} \tag{13}$$

Eq. (13) appears comparable with the Langmuir expression for the sorbed pollutant concentration (mg F per mg Al):

$$q_s = q_{\max}\frac{k\left[\text{F}\right]}{1 + K\left[\text{F}\right]} \tag{14}$$

As a matter of fact, parameter n introduced in the interpretation of EC data is analogous to the maximal amount of fluoride to be sorbed by aluminium hydroxide, $q_{\max}$, whereas specific amount q_s is related to the ratio of [Al-F] and $[\text{Al}]_t$ concentrations. This shows that the adsorption model used here is analogous to Langmuir's approach.

The above data in terms of fluoride concentrations and aluminium dosage were treated by the above model, combining the three current levels, for estimation of parameters K and n. First tests of minimisation of the objective function seemed to indicate comparable values for constant K: it has been preferred to impose the same K value for the two types of water treated, with different values for parameter n. The results reported in Fig. 9 show the good fit obtained with K = 0.389 L/mg F for the two waters, with n equal to 0.22 mg F/mg Al for deionised water and 0.68 mg F/mg Al for tap water. The different values for n correspond to the above discussed Al dosages required for EC treatment. Moreover, considering the molecular weights of fluoride and aluminium elements, n coefficient can be expressed in mol/mol, with corresponding values of 0.31 and 0.97 mol F^-/mol Al(III).

From Eq. (10), the amount of "free" Al sites is equivalent to that of complexed Al sites when product (K[F]) is equal to 1: from the estimated K value, this yields a fluoride concentration near 2.57 mg/L. From the experimental values of fluoride and Al(III) concentrations, the fraction of free Al(III) has been calculated for treatment of the two types of fluoride solutions

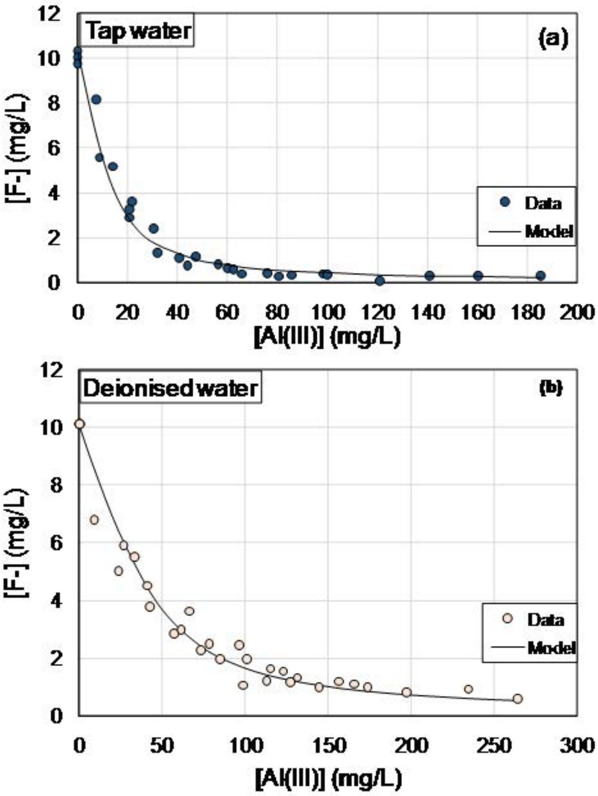

Fig. 9. Experimental and predicted profiles of fluoride concentration with various current densities (i = 2, 3, and 5 mA/cm^2) versus the concentration of dissolved aluminium generated in the EC cell: (a) tap water-based fluoride solutions and (b) deionised water-based fluoride solutions.

(Figs. 10(a) and (b)): as can be deduced by examination of Eq. (10), for low aluminium dosage, corresponding to modest fluoride abatement – [F⁻] larger than 2.57 mg/L – aluminium hydroxide sites are mostly complexed by removed fluoride. In contrast, nearly complete treatment of water requires large amounts of dissolved aluminium, for which a large fraction of sites is still available for adsorption of fluoride, according to equilibrium Eq. (10). Again, the level of Al dosages largely depends on the water quality investigated.

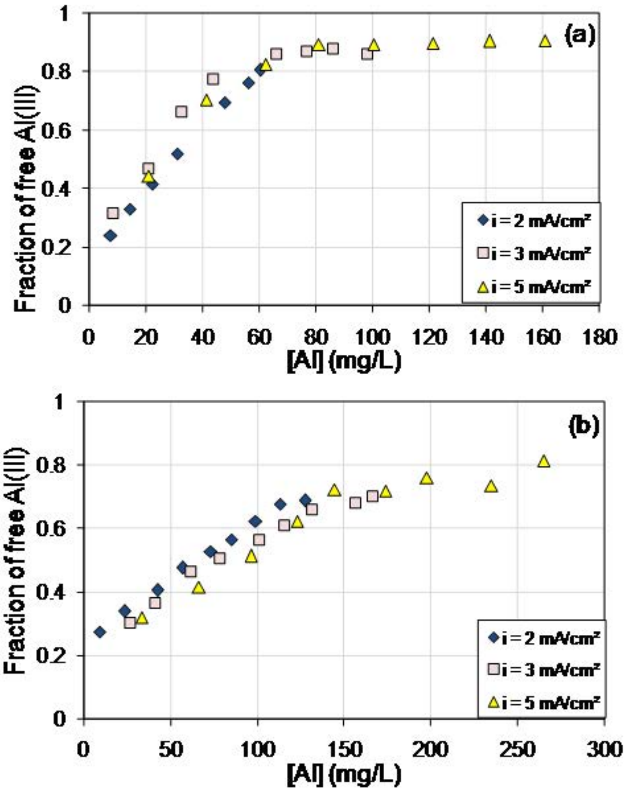

Fig. 10. Fraction of free Al(III) (calculated by the model) with various current densities (i = 2, 3, and 5 mA/cm^2) versus the concentration of dissolved aluminium generated in the EC cell: (a) tap water-based fluoride solutions and (b) deionised water-based fluoride solutions.

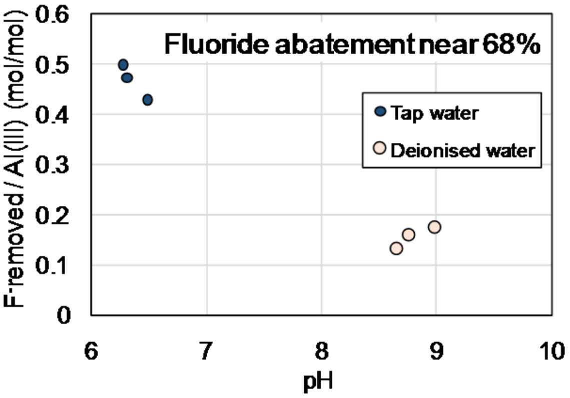

Fig. 11. Molar ratio of fluoride removed over Al(III) generated versus the solution pH for deionised and tap water-based fluoride solutions with various current densities (i = 2, 3, and 5 mA/cm^2) after abatement yield equal to 68% ± 2% (no specific symbols for the three current densities).

On a more fundamental level, as done by Hamamoto and Kishimoto [14], the molar fluoride-over-adsorbent ratio in the sludge has been estimated for a RE close to 68%: the data obtained for the three current densities and the two waters versus the solution pH are shown in Fig. 11. As observed by the two authors, this molar ratio lies between 0.4 and 0.5 for tap water, with pH ranging from 6.3 and 6.5 depending on the current density, but only between 0.1 and 0.2 upon use of deionised water, with a pH ranging from 8.6 to 9. In accordance with the above quoted paper, these results express the favoured adsorption of fluoride at moderate pH, in particular below the PZC level of solid $Al(OH)_3$ near 7.4.

4. Conclusion

The present work was aimed at investigating the removal of fluoride anions by EC, depending on the water to be treated, more precisely depending on whether the water has significant contents of chloride or hydrogen carbonate ions. Whereas the treatment of the two fluoride-containing waters can be carried out with comparable electrical charge, the amount of aluminium consumed can be dramatically different because of the cathode corrosion. In fact, the amount of aluminium dissolved in water solution depends not only on current density but also on chloride concentration. Chloride has more effect on cathode corrosion than anode. Cathode corrosion due to chloride ions seems to be more important than that induced by hydroxyl ions produced near the cathode. Hydrogen carbonate ions have a positive effect on fluoride removal by buffering the pH in the predominant area of $Al(OH)_3$ solid. However, the appreciable content of hydrogen carbonate and calcium ions induces deposition of solid calcium carbonate (calcite) on the cathode. This deposit can greatly reduce aluminium corrosion of the cathode. Therefore, for comparable treatment, the amount of aluminium sludge was largely reduced with carbonate-containing water, which reduces the aluminium plate cost and the environmental issues induced by disposal of this sludge. The fluoride removal mechanism does not only consist of the competitive adsorption between hydroxyl and fluoride but also covers the formation of solid aluminium fluoride-hydroxide $AlF_n(OH)_{3-n}$. In accordance with former works, the stoichiometry coefficient between fluoride ions and Al(III), which one can define from EC experiments, depends largely on the solution pH, consistent with the Langmuir-derived model used for interpretation of the data. In addition, because fluoride removal by adsorption on Al(III) flocs is favoured by moderate pH levels, it might now be considered to perform EC treatment upon pH control to limit the pH under 7, to increase the F-over-Al ratio in the sludge produced.

The results obtained are currently used through investigation of (i) chemical coagulation upon combined addition of Al(III) salts and alkali and (ii) continuous EC test in a cell more representative of industrial practice and comprising a settling region.

Acknowledgements

Thanks are due to the Tunisian Ministry of Higher Education and Scientific Research for funding of N. Ben Grich's PhD grant and PHC-Utique programme through 15G1119 Project. Some facilities used in the work have been funded through SusChemProc project, with the joint French Ministry of Research and Region Lorraine CPER programme (2015–2020).

Appendix

Speciation and solubility of trivalent aluminium in water

Trivalent cation of aluminium is known to undergo various hydrolysis reactions depending on the solution pH as follows:

$$\mathrm{Al}^{3+} + n\mathrm{H_2O} = \mathrm{Al(OH)}_n^{(3-n)+} + n\mathrm{H}^+ \quad \text{with equilibrium constant } K_n, \text{ for } n = 1, 4 \tag{A1}$$

At 25°C, $K_1 = 1.00 \times 10^{-5}$, $K_2 = 10^{-10.1}$, $K_3 = 10^{-16.8}$, and $K_4 = 10^{-23}(\mathrm{mol/L})^n$ [42,56–59]. Besides, H^+ and OH^- ions are in equilibria with the water. The hydrolysis constant is equal to $10^{-14}(\mathrm{mol/L})^2$ at 25°C. From the above hydrolysis reactions, the concentration of the hydroxylated forms can be expressed as functions of the concentrations of Al^{3+} species:

$$\left[\mathrm{Al}\left(\mathrm{OH}\right)_n^{(3-n)+}\right] = K_n \frac{\left[\mathrm{Al}^{3+}\right]}{\left[H^+\right]^n} \quad \text{for } n = 1,4 \tag{A2}$$

If C_t represents the total concentration of trivalent aluminium species, the mass balance on trivalent aluminium is written as:

$$C_t = \left[\mathrm{Al}^{3+}\right] + \sum_{n=1}^{4}\left[\mathrm{Al}\left(\mathrm{OH}\right)_n^{(3-n)+}\right] \tag{A3}$$

$$\text{i.e. } C_t = \left[\mathrm{Al}^{3+}\right] \times \left(1 + \sum_{n=1}^{4} \frac{K_n}{\left[\mathrm{H}^+\right]^n}\right) \tag{A4}$$

From Eq. (A4), Al^{3+} concentration can be calculated for a given value of C_t and at a given pH. The above calculations do not take into account the finite solubility of trivalent aluminium, whose solubility product K_s is equal to [60]

$$K_s = [\mathrm{Al}^{3+}]\,[\mathrm{OH}^-]^3 = 2.51 \times 10^{-32}(\mathrm{mol/L})^4 \tag{A5}$$

The upper limit of Al^{3+} concentration can be calculated from Eq. (A5) depending on pH. Therefore, the actual concentration of Al^{3+} ion is the lower value of the two estimates: (i) one deduced from Eq. (A4) and considering C_t as the total amount of Al dissolved from the metal plates and (ii) the other drawn from the solubility product. From the "real" value of soluble Al^{3+} concentration, the concentrations of the hydroxylated forms $\mathrm{Al(OH)}_n^{(3-n)+}$ can be calculated with rel. (A1), leading to the solubility of Al(III) forms, $C_{t,\mathrm{liq}}$, by using Eq. (A4). These concentrations can also be expressed in the form of mole fractions by division by the overall Al(III) concentration C_t.

References

[1] M. Mohapatra, S. Anand, B.K. Mishra, D.E. Giles, P. Singh, Review of fluoride removal from drinking water, J. Environ. Manage., 91 (2009) 67–77.

[2] C.B. Dissanayake, The fluoride problem in the ground water of Sri Lanka – environmental management and health, Int. J. Environ. Stud., 38 (1991) 137–156.

[3] E.I. Reardon, Y.X. Wang, A limestone reactor for fluoride removal from wastewaters, Environ. Sci. Technol., 34 (2000) 3247–3253.

[4] F. Shen, X. Chen, P. Gao, G. Chen, Electrochemical removal of fluoride ions from industrial wastewater, Chem. Eng. Sci., 58 (2003) 987–993.

[5] Q. Guo, Q. Guo, Water defluoridation by hydrotalcite and takovite and subsequent formation of new fluoride-bearing phases, Environ. Technol., 34 (2013) 1053–1062.

[6] E. Mulugeta, F. Zewge, C.A. Johnson, B.S. Chandravanshi, Aluminium hydro(oxide)–based (AO) adsorbent for defluoridation of drinking water: optimisation, performance comparison, and field testing, Water SA, 41 (2015) 121–128.

[7] WHO (World Health Organization), Guidelines for Drinking Water Quality, Recommendations, 3rd ed., World Health Organization, Geneva, 2004.

[8] J. Fawell, K. Bailey, J. Chilton, E. Dahi, L. Fewtrell, Y. Magara, Fluoride in Drinking-water, World Health Organization (WHO) ISBN: 1900222965 (2006), Published by IWA Publishing, London, UK, 2006.

[9] USPHS (United States Public Health Service) Drinking Water Standards, US Government Printing Office, Department of Health Education and Welfare, Washington, DC, 1962.

[10] Meenakshi, R.C. Maheshwari, Fluoride in drinking water and its removal, J. Hazard. Mater., B137 (2006) 456–463.

[11] J.J. Schoeman, Performance of a water defluoridation plant in a rural area in South Africa, Water SA., 35 (2009) 97–101.

[12] N. Mameri, A.R. Yeddou, H. Lounici, D. Belhocine, H. Grib, B. Bariou, Defluoridation of septentrional Sahara water of North Africa by electrocoagulation process using bipolar aluminium plates, Water Res., 32 (1998) 1604–1612.

[13] R. Sinha, S. Mathur, U. Brighu, Aluminum removal from water after defluoridation with the electrocoagulation process, Environ. Technol., 36 (2015) 2724–2731.

[14] S. Hamamoto, N. Kishimoto, Characteristics of fluoride adsorption onto aluminium(III) and iron(III) hydroxide flocs, Sep. Sci. Technol., 52 (2017) 42–50.

[15] A. Ben Nasr, C. Charcosset, R. Ben Amar, K. Walha, Fluoride removal from aqueous solution by Purolite A520E resin: kinetic and thermodynamics study, Desal. Wat. Treat., 54 (2015) 1604–1611.

[16] A. Toyoda, T. Taira, A new method for treating fluorine wastewater to reduced sludge and running costs, IEEE Trans. Semicond. Manuf., 13 (2000) 305–309.

[17] S. Aoudj, A. Khelifa, N. Drouich, R. Belkada, D. Miroud, Simultaneous removal of chromium(VI) and fluoride by electrocoagulation-electroflotation: application of a hybrid Fe-Al Anode, Chem. Eng. J., 267 (2015) 153–162.

[18] T. Ouslimane, S. Aoudj, M. Amara, N. Drouiche, Removal of copper and fluoride from mixed Cu-CMP and fluoride-bearing wastewaters by electrocoagulation, Int. J. Environ. Res., 11 (2017) 677–684.

[19] K.M. Popat, P.S. Anand, B.D. Dasare, Selective removal of fluoride ion from water by the aluminium from of the aminomethylphosphonic acid type ion exchange, React. Polym., 23 (1994) 23–32.

[20] S. Meenakshi, N. Viswanathan, Identification of selective ion-exchange resin for fluoride sorption, J. Colloid Interface Sci., 308 (2007) 438–450.

[21] M.F. Chang, J.C. Liu, Precipitation removal of fluoride from semiconductor waste water, J. Environ. Eng., 33 (2007) 419–525.

[22] A. Mazighi, H. Lounichi, N. Drouich, R. Leenaerts, N. Abdi, H. Grib, N. Memeri, Economic study of groundwater defluoridation of the North African Sahara, Desal. Wat. Treat., 54 (2014) 2681–2691.

[23] M. Bennajah, M. Maalmi, Y. Darmane, M. Ebn Touhaim, Defluoridation of drinking water by electrocoagulation/electroflotation: kinetic study, J. Urban Environ. Eng., 4 (2010) 36–44.

[24] A. Attour, M. Touati, M. Tlili, M. Ben Amor, F. Lapicque, J.P. Leclerc, Influence of operating parameters on phosphate removal from water by electrocoagulation using aluminium electrodes, Sep. Purif. Technol., 123 (2014) 124–129.

[25] A. Attour, N. Ben Grich, M. Tlili, M. Ben Amor, F. Lapicque, J.P. Leclerc, Intensification of phosphate removal using electrocoagulation treatment by continuous pH adjustment and optimal electrode connection mode, Desal. Wat. Treat., 57 (2016) 13255–13262.

[26] T. Picard, G. Cathalifaud-Feuillade, M. Mazet, C. Vandensteendam, Cathodic dissolution in the electrocoagulation process using aluminium electrodes, J. Environ. Monit., 2 (2000) 77–80.

[27] P. Canizares, M. Carmona, J. Lobato, F. Martinez, M.A. Rodrigo, Electrodissolution of aluminium electrodes in electrocoagulation processes, Ind. Eng. Chem. Res., 44 (2005) 4178–4185.

[28] P.K. Holt, G.W. Barton, C.A. Mitchell, The future for electrocoagulation as a localised water treatment technology, Chemosphere, 59 (2005) 355–367.

[29] A.S. Koparal, U. Bakir, U.B. Ogutveren, Removal of nitrate from water by electroreduction and electrocoagulation, J. Hazard. Mater., 89 (2002) 83–94.

[30] K.S. Hashim, A. Shaw, R. Al Khaddar, M.O. Pedro, Energy efficient electrocoagulation using a new flow column reactor to remove nitrate from drinking water-experimental, statistical, and economic approach, J. Environ. Manage., 196 (2017) 224–233.

[31] D. Xu, Y. Li, L. Yin, Y. Ji, J. Niu, Y. Yu, Electrochemical removal of nitrate in industrial wastewater, Front. Environ. Sci. Eng., 12 (2018) 1–14.

[32] S. Vasudevan, J. Lakshmi, G. Sozhan, Studies on a Mg-Al-Zn Alloy as an anode for the removal of fluoride from drinking water in an electrocoagulation process, CLEAN–Soil Air Water, 37 (2009) 372–378.

[33] B. Palahouane, N. Drouiche, K. Bensadok, S. Aoudj, M. Hecini, A remediation of post treated fluorinated photovoltaic wastewater by electrocoagulation, Chem. Eng. Trans., 32 (2013) 25–30.

[34] N. Mameri, H. Lounici, D. Belhocine, H. Grib, D.L. Piron, Y. Yahiat, Defluoridation of Sahara water by small plant electrocoagulation using bipolar aluminium electrodes, Sep. Purif. Technol., 24 (2001) 113–119.

[35] N. Drouiche, S. Aoudj, M. Hecini, N. Ghaffour, H. Lounici, N. Mameri, Fluoride removal with aluminium electrodes–Characteristics of products, J. Hazard. Mater., 169 (2009) 65–69.

[36] S. Aoudj, A. Khelifa, N. Drouich, M. Hecini, Removal of fluoride and turbidity from semiconductor industry wastewater by combined coagulation and electroflotation, Desal. Wat. Treat., 57 (2015) 18398–18405.

[37] J.E. Van Benschoten, J.K. Edzwald, Chemical aspects of coagulation using aluminium salts—I. Hydrolytic reactions of alum and polyaluminium chloride, Water Res., 24 (1990) 1519–1526.

[38] C.Y. Hu, S.L. Lo, W.H. Kuan, Effects of the molar ratio of hydroxide and fluoride to Al(III) on fluoride removal by coagulation and electrocoagulation, J. Colloid Interface Sci., 283 (2005) 472–476.

[39] C.Y. Hu, S.L. Lo, W.H. Kuan, Simulation the kinetics of fluoride removal by elecrocagulation (EC) process using aluminium electrodes, J. Hazard. Mater., 145 (2007) 180–185.

[40] M. Bennajah, B. Gourich, A.H. Essadki, Ch. Vial, H. Delmas, Defluoridation of Morocco drinking water by electrocoagulation/electroflottation in an electrochemical external-loop airlift reactor, Chem. Eng. J., 148 (2009) 122–131.

[41] A.H. Essadki, B. Gourich, Ch. Vial, H. Delmas, M. Bennajah, Defluoridation of drinking water by electrocoagulation/electroflotation in a stirred tank reactor with a comparative performance to an external-loop airlift reactor, J. Hazard. Mater., 168 (2009) 1325–1333.

[42] U. Ntuk, S. Tait, E.T. White, K.M. Steel, The precipitation and solubility of aluminium hydroxyfluoride hydrate between 30 and 70°C, Hydrometallurgy, 155 (2015) 79–87.

[43] J. Zhu, H. Zhao, J.-R. Ni, Fluoride distribution in electrocoagulation defluoridation process, Sep. Purif. Technol., 56 (2007) 184–191.

[44] M.G. Sujana, R.S. Thakur, S.B. Rao, Removal of fluoride from aqueous solutions by using aluminium sludge, J. Colloid Interface Sci., 206 (1998) 94–101.

[45] H.-Z. Zhao, W. Yang, J. Zhu, J.-R. Ni, Defluoridation of drinking water by combined electrocoagulation: effects of the molar ratio of alkalinity and fluoride to Al(III), Chemosphere, 74 (2009) 1391–1395.

[46] A.E. Greenberg, L.S. Clesceri, A.D. Eaton, Standard Methods: For the Examination of Water and Wastewater, 18th ed., APHA, Washington, DC, 1992.

[47] Afnor (Agence Française de Normalisation), Qualité de l'eau, Recueil des normes françaises, 2nd ed., vol. 3, Paris, 1997 [in French].

[48] J. Rodier, L'analyse de l'eau, 9th ed., Dunod, Paris, 2009.

[49] V. Landolt, Traité des Matériaux: Corrosion et Chimie de Surface des Métaux, Presse Polytechniques et Universitaires Romandes, Lausanne, 1993.

[50] D.L. Parkhurst, C.A.J. Appelo, Description of input and examples for PHREEQC version 3- A computer program for speciation, batch reaction, one-dimensional transport and inverse geochemical calculations, US Geological Survey Techniques and Methods, Book 6, Chap., A43, 2013.

[51] K. Govindan, M. Raja, S.U. Maheshwari, M. Noel, Y. Oren, Comparison and understanding of fluoride removal mechanism in Ca^{2+}, Mg^{2+} and Al^{3+} ion assisted electrocoagulation process using Fe and Al electrodes, J. Environ. Chem. Eng., 3 (2015) 1784–1793.

[52] Q. Zuo, X. Chen, W. Li, G. Chen, Combined electrocoagulation and electroflotation for removal of fluoride from drinking water, J. Hazard. Mater., 159 (2008) 452–457.

[53] M.M. Emamjomeh, M. Sivakumar, Fluoride removal by a continuous flow electrocoagulation reactor, J. Environ. Manage., 90 (2009) 1204–1212.

[54] A.H. Essadki, B. Gourich, M. Azzi, Ch. Vial, H. Delmas., Kinetic study of defluoridation of drinking water by electrocoagulation/electroflotation in a stirred tank reactor and in an external-loop airlift reactor, Chem. Eng. J., 164 (2010) 106–114.

[55] M. Khemis, J.P. Leclerc, G. Tanguy, G. Valentin, F. Lapicque, Treatment of industrial liquid wastes by electrocoagulation: experimental investigations and an overall interpretation model, Chem. Eng. Sci., 61 (2006) 3602–3609.

[56] J.W. Ball, D.K. Nordstrom, E.A. Jenne, Additional and revised thermochemical data and computer code for WAT Q2: a computerized chemical model for trace and major element speciation and mineral equilibria of natural waters, Water-Resources Investigations Report, U.S. Geological Survey, 1980, pp. 78–116.

[57] S.P. Bi, S.Q. An, W. Tang, M. Yang, H.F. Qian, J. Wang, Modeling the distribution of aluminium speciation in acid soil solution equilibria with the mineral phase alunite, Environ. Geol., 41 (2001) 25–36.

[58] D.F. Lisbona, K.M. Steel, Recovery of fluoride values from spent pot-lining: Precipitation of an aluminium hydroxyfluoride hydrate product, Sep. Purif. Technol., 61 (2008) 182–192.

[59] S. George, P. Pandit, A.B. Gupta, Residual aluminium in water defluoridated using activated alumina adsorption – Modeling and simulation studies, Water Res., 44 (2010) 3055–3064.

[60] J.E. Van Benschoten, J.K. Edzwald, Chemical aspects of coagulation using, Aluminum salts—I. Hydrolytic reactions of Alum and polyaluminum chloride, Water Res., 24 (1990) 1519–1526.